Young's modulus of graphene: A molecular dynamics study

Jin-Wu Jiang,[1] Jian-Sheng Wang,[1] and Baowen Li[1,2]

[1]*Department of Physics and Centre for Computational Science and Engineering, National University of Singapore,*
Singapore 117542, Republic of Singapore
[2]*NUS Graduate School for Integrative Sciences and Engineering, Singapore 117456, Republic of Singapore*

The Young's modulus of graphene is investigated through the intrinsic thermal vibration in graphene which is "observed" by molecular dynamics and the results agree very well with the recent experiment [Lee *et al.*, Science **321**, 385 (2008)]. This method is further applied to show that the Young's modulus of graphene (1) increases with increasing size and saturates after a threshold value of the size; (2) increases from 0.95 to 1.1 TPa as temperature increases in the region [100, 500] K; (3) is insensitive to the isotopic disorder in the low disorder region (<5%) and decreases gradually after further increasing the disorder percentage.

The single-layer graphene has unique electronic and other physical properties thus becoming a promising candidate for various device applications.[1,2] Among others, excellent mechanical property is an important advantage for the practical applications of graphene. Experimentally, the Young's modulus (Y) of graphene has been measured by using atomic force microscope (AFM) to introduce external strain on graphene and record the force-displacement relation.[3] The measured value for Young's modulus is 1.0 ± 0.1 TPa in this experiment. Theoretically, the Young's modulus of graphene can be studied in a parallel way. Once the external strain is applied on graphene, the internal force or potential can be calculated in different approaches, such as *ab initio* calculations,[4–6] molecular dynamics (MD),[7] and interatomic potentials.[8–10] Then the Young's modulus can be obtained from the force-displacement or the potential-displacement relation. For the carbon nanotubes (CNT), the Young's modulus is theoretically studied in a similar way as that in graphene. However, in the experiment, besides the AFM method,[11] another group measured the Young's modulus of CNT by observing the thermal vibration at the tip of the CNT using the transmission electron microscopy (TEM).[12,13] For some unknown reasons, possibly technical challenges, this experimental method does not appear in the study of the Young's modulus in graphene. As a supplement to this vacancy, the present work "observes" the thermal vibration of graphene by MD instead of TEM and then calculates the Young's modulus from the "observed" thermal vibration.

In the engineering application of graphene, it will be beneficial if the mechanical property of graphene can be adjusted according to the demand. There are some possible methods that can manipulate the value of Young's modulus in graphene, such as size of the sample, temperature, isotopic disorder, etc. It is a matter of practical importance and theoretical interest to find an effective method to control the mechanical property of graphene. The present calculation method for the Young's modulus of graphene in this paper is readily applicable to address these issues.

In this Brief Report, we investigate the Young's modulus of graphene by observing the thermal vibrations with MD. The calculated Young's modulus is in good agreement with the recent experimental one. Using this method, we can systematically study different effects on the Young's modulus:

size, temperature, and isotopic disorder. It shows that the Young's modulus increases as graphene size increases and saturates. In the temperature range 100–500 K, Y increases from 0.95 to 1.1 TPa as T increases. For the isotopic disorder effect, Y keeps almost unchanged within low disorder percentage (<5%) and decreases gradually after further increasing disorder percentage.

In graphene there are both optical and acoustic vibration modes in the z direction. For the optical phonon modes, the frequency is about 850 cm^{-1}, which is too high to be considerably excited under 500 K. While the acoustic phonon mode is a flexure mode with parabolic dispersion $\omega = \beta k^2$, which will be fully excited even at very low temperature. So the thermal mean-square vibration amplitude (TMSVA) of graphene in the z direction is mainly attributed to the flexure mode under 500 K. In this sense, we consider the contribution of the flexure mode to TMSVA for an elastic plate in the following. The x and y axes lie in the plate, and z direction is perpendicular to the plate. For convenience and without losing generality, we consider a square plate with length L.

The equation for oscillations in z direction of a plate is[14]

$$\rho \frac{\partial^2 z}{\partial t^2} + \frac{D}{h}\Delta^2 z = 0, \qquad (1)$$

where $D = \frac{1}{12} Y h^3/(1-\mu^2)$. Δ is the two-dimensional Laplacian and ρ is the density of the plate. Y and μ are the Young's modulus and the Poisson ratio, respectively. h is the thickness of the plate. We apply fixed boundary condition in x direction and periodic boundary condition in y direction:

$$z(t, x=0, y) = 0,$$

$$z(t, x=L, y) = 0,$$

$$z(t, x, y+L) = z(t, x, y). \qquad (2)$$

The solution for the above partial differential equation under these boundary conditions can be found in Ref. 15:

$$\omega_n = k_n^2 \sqrt{\frac{Yh^2}{12\rho(1-\mu^2)}},$$

$$z_n(t,x,y) = u_n \sin(k_1 x) \cos(k_2 y) \cos(\omega_n t),$$

$$\vec{k} = k_1 \vec{e}_x + k_2 \vec{e}_y, \tag{3}$$

where $k_1 = \pi n_1 / L$ and $k_2 = 2\pi n_2 / L$.

Using these eigensolution, the TMSVA for nth phonon mode in (x,y) at temperature T can be obtained:[13]

$$\sigma_n^2(x,y) = 4k_B T \frac{12(1-\mu^2)}{Yh^2 V} \frac{1}{k_n^4} [\sin(k_1 x)\cos(k_2 y)]^2. \tag{4}$$

We should mention that for those modes with $k_1 \neq 0$ and $k_2 = 0$, we have a similar result $\sigma_n^2(x,y) = 2k_B T \frac{12(1-\sigma^2)}{Eh^2 V} \frac{1}{k_n^4}(\sin k_1 x)^2$. The spatial average of the TMSVA over x and y is

$$\langle \sigma_n^2 \rangle = \frac{1}{S} \int \int_D \sigma_n^2(x,y)dxdy = k_B T \frac{12(1-\mu^2)}{Yh^2 V} \frac{1}{k_n^4}, \tag{5}$$

where $k_1 \neq 0$ and $k_2 \neq 0$. D is the field in $x \in [0,L]$ and $y \in [0,L]$, and $S = L^2$ is the area of D. If $k_1 \neq 0$ and $k_2 = 0$, $\langle \sigma_n^2 \rangle$ turns out to have the same expression as this general one.

Because all modes are independent at the thermal equilibrium state at temperature T, they contribute to the TMSVA incoherently. As a result, the TMSVA at temperature T is given by

$$\langle \sigma^2 \rangle = \sum_{n=0}^{\infty} \langle \sigma_n^2 \rangle$$

$$= k_B T \frac{12(1-\mu^2)}{Yh^2 V} \sum_{n=0}^{\infty} \frac{1}{k_n^4}$$

$$= k_B T \frac{12(1-\mu^2)}{Yh^2 V} \frac{2S^2}{\pi^4} C$$

$$= 0.31 \frac{(1-\mu^2)S}{h^3} \frac{k_B T}{Y}. \tag{6}$$

The constant $C = \sum_{n_1=1}^{+\infty} \sum_{n_2=0}^{+\infty} \epsilon_{n_2} \frac{1}{(n_1^2 + 4n_2^2)^2} \approx 1.2507$, the major part of which is due to the first nonzero phonon mode with $(n_1, n_2) = (1,0)$. $\epsilon_{n_2} = 1$ for $n_2 = 0$ and $\epsilon_{n_2} = 2$ for other $n_2 = 1, 2, 3, \ldots$.

As a result, the Young's modulus of the graphene is

$$Y = 0.3 \frac{S}{h^3} \frac{k_B T}{\langle \sigma^2 \rangle}. \tag{7}$$

The Poisson ratio in graphene[16,17] $\mu = 0.17$ has been used in this expression for the Young's modulus. There is arbitrariness in the definition of thickness h of the one-atom-thick graphene sheet. For convenience of comparison between our theoretical results and the experimental ones, we choose h to be 3.35 Å, the interlayer space in graphite, which is also used in the experimental work.[3]

Figure 1 is the configuration of the graphene sheet in our simulation. The outmost two columns (red online) on the left
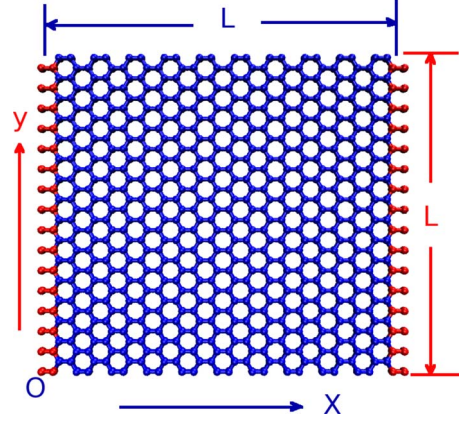

FIG. 1. (Color online) Configuration of the graphene sample. The origin O is at the left bottom of the sample. Two columns (red online) on the left and right sides are fixed. The length of the sample in this figure is $L=40$ Å.

and right sides are fixed during the simulation while periodic boundary condition is imposed in the vertical direction. The origin of the coordinate is set at the left bottom of the sample. The x axis is in the horizontal direction and y axis is in the vertical direction.

The MD simulations are performed using the second-generation Brenner interatomic potential.[18] The Newton equations of motion are integrated within the fourth order Runge-Kutta algorithm, in which a time step of 0.5 fs is applied. The typical MD simulation steps in this paper is 5×10^5, corresponding to 0.25 ns simulation time.

The initial velocities of carbon atoms at temperature T are assigned as independent Gaussian random variables drawn from the Maxwell-Boltzmann distribution. All atoms are at the optimized position at $t=0$. A long enough simulation time is used for the system to reach steady state. In our simulation, 5×10^5 MD steps are used to ensure that the system has achieved the thermal equilibrium. Another 5×10^5 MD steps are applied to calculate the time-averaged quantities in this Brief Report. The typical variation in the total energy of the system is very small ($<2\%$).

After obtaining the $\langle \sigma^2 \rangle$ from MD simulation, we can calculate the value of Young's modulus through Eq. (7). We note that the elastic theory has been successfully applied to describe atomic graphene system with about 400 carbon atoms.[19] In this Brief Report, the graphene samples have about 200–500 carbon atoms. So we expect the Eq. (7) resulted from elastic theory can also be applicable. To depress the possible error created by randomness in the simulation, we repeat 100 independent processes for each value of the Young's modulus in this work.

Figure 2 shows the size dependence of the Young's modulus. When 10 Å $< L <$ 40 Å, Y increases from 0.7 to 1.1 TPa with increasing size, and this value (1.1 TPa) almost does not change with further increasing L. The increase in Y with increasing size also shows up in some studies on the Young's modulus of CNT by various methods, where Y increases with increasing diameter and reaches a saturate value.[20–23] In Fig. 2, the value of Y in large size sample is 1.1 TPa. This value agrees quite well with the recent experimental 1 ± 0.1 TPa result.[3]
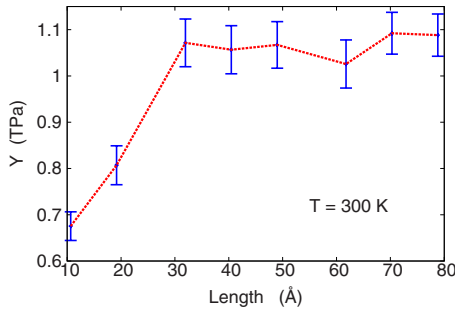
FIG. 2. (Color online) The Young's modulus in graphene with different sizes.

In Fig. 3, we show the temperature dependence of the Young's modulus in the temperature range from 100 to 600 K. In the low-temperature region [100, 500] K, Y increases for 15% as T increases. In the high-temperature region $T > 500$ K, Y shows obvious decreasing behavior. This behavior indicates that the suitable temperature region for our method is $T < 500$ K. If $T > 500$ K, the optical phonon modes in the z direction will also be excited together with the flexure mode, leading to a larger value for the TMSVA in our MD simulation. And the result from Eq. (7) will underestimate the value of Young's modulus.

Now we consider the result of the ^{14}C isotopic disorder in the pure ^{12}C graphene system. We expect this investigation of the isotopic disorder effect can give a useful clue to whether mechanical properties of graphene can be manipulated in this way. In our simulation, to calculate the value of Y under a particular isotopic disorder percentage, ^{12}C atoms are randomly substituted by certain number of ^{14}C atoms. This procedure is done independently in each of our 100 simulation processes for one value of the Young's modulus. Results are shown in Fig. 4. We find that the value of Y remains almost unchanged for the low isotopic disorder percentage ($<5\%$). Further increase of the isotopic disorder percentage yields about 15% reduction in Y. This result tells us that the purification of the natural graphene cannot obtain a higher value of Y. On the other hand, about 15% reduction in Y can be realized by increasing the isotopic disorder percentage. However, as 20% isotopic disorder only achieves 15% reduction in Y, it is not an effective method to control the value of Y by modifying isotopic disorder percentage. This situation is very different from that in the thermal transport.
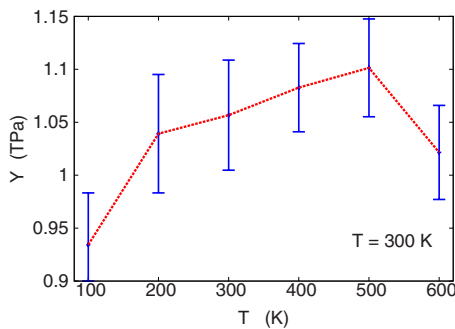

FIG. 3. (Color online) The dependence of the Young's modulus on temperature T for graphene with $L = 40$ Å.
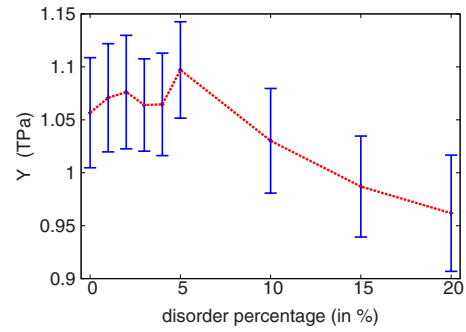

FIG. 4. (Color online) The isotopic disorder effect on the Young's modulus of graphene at $T = 300$ K with $L = 40$ Å.

The thermal conductivity has been shown to be very sensitive to the isotopic disorder percentage in the low disorder region with more than 40% reduction in thermal conductivity by less than 5% isotopic disorder percentage; while for higher disorder percentage, the thermal conductivity keeps almost unchanged.[24–26] So the thermal conductivity can be greatly enhanced by synthesizing isotropically pure nanotubes.[26]

In conclusion, we have used MD to obtain the thermal vibration of graphene and then calculate the Young's modulus from the thermal mean-square vibration amplitude. The advantage of this approach is that we don't have to introduce external strain on the system and it can be easily applied to study different effects on the Young's modulus. The theoretical results agree very well with the experimental ones. As an application of this method, we study the Young's modulus of graphene with different size. The temperature and isotopic disorder effects on the Young's modulus are also investigated. It shows that the Young's modulus increases with increasing size when the graphene sample is smaller than 40 Å and reaches a saturated value in samples larger than 40 Å. The value of Y increases from 0.95 to 1.1 TPa as T increases from 100 to 500 K. For the isotopic disorder effect, Y keeps almost unchanged in the low disorder region ($<5\%$) and decreases gradually for 15% after increasing the disorder percentage up to 20%. This finding provides the information that the isotopic disorder is not an effective method to control the Young's modulus of graphene.

We should point out that why we use the constant value of Poisson ratio $\mu = 0.17$. Actually μ also depends on the size, temperature, and isotopic doping. By applying external strain (ε_x) on the graphene in x direction, and using MD to record the resulted strain in y direction (ε_y) under different environment, i.e., different size, temperatures, or isotopic doping percentage, we can obtain the value of Poisson ratio from $\mu = |\varepsilon_y / \varepsilon_x|$. We find that the value of Poisson ratio will deviate from 0.17, which means that it will introduce some error if we use a constant value for Poisson ratio under all environment. However, as can be seen from Eq. (6), the Poisson ratio appears in the expression as a factor $(1 - \mu^2)$, so the error is considerably small. For example, we find that the largest value for Poisson ratio is 0.22 in graphene sheet with

$L=10$ Å at 300 K without isotopic doping. In this situation, the relative error is the largest, which is $[(1-0.22^2)-(1-0.17^2)]/(1-0.17^2)=-2\%$. So throughout this Brief Report, we use a constant value for Poisson ratio, which will introduce relative error for the Young's modulus less than 2%.

[1] A. K. Geim and K. S. Novoselov, Nature Mater. **6**, 183 (2007).

[2] A. H. Castro Neto, F. Guinea, N. M. R. Peres, K. S. Novoselov, and A. K. Geim, Rev. Mod. Phys. **81**, 109 (2009).

[3] C. G. Lee, X. D. Wei, J. W. Kysar, and J. Hone, Science **321**, 385 (2008).

[4] K. N. Kudin, G. E. Scuseria, and B. I. Yakobson, Phys. Rev. B **64**, 235406 (2001).

[5] G. Van Lier, C. Van Alsenoy, V. Van Doren, and P. Geerlings, Chem. Phys. Lett. **326**, 181 (2000).

[6] E. Konstantinova, S. O. Dantas, and P. M. V. B. Barone, Phys. Rev. B **74**, 035417 (2006).

[7] R. Khare, S. L. Mielke, J. T. Paci, S. Zhang, R. Ballarini, G. C. Schatz, and T. Belytschko, Phys. Rev. B **75**, 075412 (2007).

[8] C. D. Reddy, S. Rajendran, and K. M. Liew, Nanotechnology **17**, 864 (2006).

[9] Y. Huang, J. Wu, and K. C. Hwang, Phys. Rev. B **74**, 245413 (2006).

[10] J. P. Lu, Phys. Rev. Lett. **79**, 1297 (1997).

[11] T. W. Tombler, C. Zhou, L. Alexseyev, J. Kong, H. Dai, L. Liu, C. S. Jayanthi, M. Tang, and S. Y. Wu, Nature (London) **405**, 769 (2000).

[12] M. M. J. Treacy, T. W. Ebbesen, and J. M. Gilson, Nature (London) **381**, 678 (1996).

[13] A. Krishnan, E. Dujardin, T. W. Ebbesen, P. N. Yianilos, and M. M. J. Treacy, Phys. Rev. B **58**, 14013 (1998).

[14] L. D. Landau and E. M. Lifshitz, *Theory of Elasticity* (Pergamon, Oxford, 1995).

[15] A. D. Polyanin, *Handbook of Linear Partial Differential Equations for Engineers and Scientists* (CRC/C&H, Florida, 2002).

[16] O. L. Blakslee, D. G. Proctor, E. J. Seldin, G. B. Spence, and T. Weng, J. Appl. Phys. **41**, 3373 (1970).

[17] D. Sanchez-Portal, E. Artacho, J. M. Soler, A. Rubio, and P. Ordejón, Phys. Rev. B **59**, 12678 (1999).

[18] D. W. Brenner, O. A. Shenderova, J. A. Harrison, S. J. Stuart, B. Ni, and S. B. Sinnott, J. Phys.: Condens. Matter **14**, 783 (2002).

[19] E. Cadelano, P. L. Palla, S. Giordano, and L. Colombo, Phys. Rev. Lett. **102**, 235502 (2009).

[20] D. H. Robertson, D. W. Brenner, and J. W. Mintmire, Phys. Rev. B **45**, 12592(R) (1992).

[21] T. Chang, J. Geng, and X. Guo, Appl. Phys. Lett. **87**, 251929 (2005).

[22] J. B. Wang, X. Guo, H. W. Zhang, L. Wang, and J. B. Liao, Phys. Rev. B **73**, 115428 (2006).

[23] V. N. Popov, V. E. Van Doren, and M. Balkanski, Phys. Rev. B **61**, 3078 (2000).

[24] T. R. Anthony, W. F. Banholzer, J. F. Fleischer, L. Wei, P. K. Kuo, R. L. Thomas, and R. W. Pryor, Phys. Rev. B **42**, 1104 (1990).

[25] G. Zhang and B. Li, J. Chem. Phys. **123**, 114714 (2005).

[26] C. W. Chang, A. M. Fennimore, A. Afanasiev, D. Okawa, T. Ikuno, H. Garcia, D. Li, A. Majumdar, and A. Zettl, Phys. Rev. Lett. **97**, 085901 (2006).